

ANALYSIS OF AN ADAPTIVE DETECTION ALGORITHM FOR NON-HOMOGENEOUS ENVIRONMENTS

Christ D. Richmond

Massachusetts Institute of Technology
Lincoln Laboratory
244 Wood St., Rm J118-D
Lexington, MA 02173, USA

ABSTRACT

The adaptive matched filter (AMF) detector is known to be highly vulnerable to jammers and clutter discretions on which it has not properly trained. A vulnerability often leading to impractical false alarm rates in non-homogeneous environments. Sequentially following the AMF test with the adaptive cosine estimator (ACE) detector was proposed as a method of regulating the AMF's high false alarm rate. The overall detection algorithm, called the adaptive sidelobe blanker (ASB), is two dimensional and has exhibited significant potential in experimental settings of inhomogeneous environments. The goal of this paper is to theoretically examine the potential of this algorithm for application in non-homogeneous environments.

1. INTRODUCTION

The AMF is a constant false alarm rate (CFAR) detector under homogeneous clutter conditions and complex Gaussian statistics [8]. In practice, the inhomogeneity of radar clutter (especially in airborne radar systems), and the resulting difficulties in estimating the data covariance matrix significantly frustrate the AMF's inherent CFAR property. Essentially an adaptive beamformer the AMF suppresses clutter and interference based on an estimate of the data covariance matrix. The data covariance is typically estimated from a secondary data set or training set, which excludes the target test cell [1]. If the statistics of this training data do not characterize those of the target cell, for example the average power in the training samples may be significantly lower than the power in the test cell, then there is potentially a greater chance of experiencing many false alarms due to undernulling clutter and/or clutter discretions [2]. An adaptive detection algorithm called the *adaptive sidelobe blanker* (ASB) was proposed [2] to reduce this false alarm rate while maintaining detectability of true targets.

The ASB detection algorithm is a two stage adaptive sequential detector consisting of a first stage AMF detection followed by a second stage detector known as an *adaptive cosine estimator* (ACE) [3]. For a given test cell the AMF

statistic provides a measure of the power originating from the assumed target direction. The ACE statistic determines what fraction of the total energy present in a test cell originates from the target direction. Only range-Doppler test cells surviving both detection thresholdings are declared target bearing. The ASB has exhibited significant potential in experimental settings [2, 10, 9]. The theoretical analysis of this 2-D algorithm, which is illustrated in fig(1), under non-homogeneous conditions is the goal of this paper.

Assuming complex Gaussian statistics exact novel closed form expressions for the resulting probability of detection (PD) and probability of false alarm (PFA) for the ASB adaptive detection algorithm are derived which demonstrate that (i) the ASB has a higher or commensurate PD for a given PFA than both the AMF and the ACE, (ii) the ASB has a lower or commensurate PFA for a given PD than both the AMF and the ACE, (iii) the ASB has an overall performance which is commensurate with the benchmark *generalized likelihood ratio test* (GLRT) [1], and (iv) the ASB is computationally more efficient than a straight GLRT and provides an adjustable sensitivity to sidelobe targets.

The last section briefly discusses the viability of a constraint which made the present analysis under non-homogeneous conditions tractable and shows potential for further application in adaptive processing. The constraint is a generalized eigen-relation (GER) between the covariance of the test cell, that of the training set samples, and the target array response vector.

2. ADAPTIVE DETECTION

2.1. Problem Statement

Signal presence is sought in a $N \times 1$ vector observation (or *snapshot*) \mathbf{x} called the *test cell*. The test cell's covariance, denoted by \mathbf{R}_T , is assumed unknown. It is desired to classify this snapshot into one of two categories:

$$\begin{aligned} H_0 &: \mathbf{x} = \mathbf{n} \\ H_1 &: \mathbf{x} = S\mathbf{v} + \mathbf{n}; \end{aligned} \quad (1)$$

noise only (denoted by the hypothesis H_0), or target signal plus noise (denoted by H_1). The target array response vector is denoted by \mathbf{v} and assumed to be a known quantity. S is the target complex amplitude, which we assume deterministic yet unknown.

There are two unknown parameters, \mathbf{R}_T and S , which necessitate the use of adaptive methods. A *secondary data*

The author is with MIT Lincoln Laboratory, Lexington, MA 02173; christ@ll.mit.edu. This work was sponsored by DARPA under Air Force contract F19628-95-C-0002. Opinions, interpretations, conclusions, and recommendations are those of the author and are not necessarily endorsed by the United States Air Force.

set (or training set) consisting of L data samples ($L \geq N$) $\mathbf{X} = [\mathbf{x}_1 | \dots | \mathbf{x}_L]$ is typically acquired. Each training snapshot \mathbf{x}_i is assumed zero mean noise only, *s.t.* $\text{cov}(\mathbf{x}_i) = \mathbf{R}$ for $i = 1, \dots, L$. For the *homogeneous* clutter case we assume that $\mathbf{R}_T = \mathbf{R}$, and hence, the utility of the training set for parameter estimation [1]–[3]. Reality, however, often precludes this assumption. In this present study it is therefore of interest to likewise consider the *inhomogeneous* case in which $\mathbf{R}_T \neq \mathbf{R}$.

2.2. Detection Algorithms

The adaptive detection algorithms under consideration include the AMF, the ACE, the GLRT, and the two dimensional ASB. Define the symbol

$$\hat{\mathbf{R}} \triangleq \mathbf{X}\mathbf{X}^H, \quad (2)$$

to be the noise only (unnormalized) sample covariance matrix (SCM). The three aforementioned 1-D adaptive detectors are given by:

Adaptive Detectors

$$t_{AMF} = \frac{|\mathbf{v}^H \hat{\mathbf{R}}^{-1} \mathbf{x}|^2}{\mathbf{v}^H \hat{\mathbf{R}}^{-1} \mathbf{v}} \quad t_{ACE} = \frac{t_{AMF}}{\mathbf{x}^H \hat{\mathbf{R}}^{-1} \mathbf{x}} \quad (3)$$

$$t_{GLRT} = \frac{t_{AMF}}{1 + \mathbf{x}^H \hat{\mathbf{R}}^{-1} \mathbf{x}}.$$

Each 1-D algorithm consists of computing and thresholding a data dependent decision statistic to determine target presence. By construction $t_{AMF} \geq 0$, $0 \leq t_{GLRT} \leq 1$, and $0 \leq t_{ACE} \leq 1$. Thus, the choice of detection thresholds must reflect these bounds: $\eta_{amf} \geq 0$, $0 \leq \eta_{glrt} \leq 1$, and $0 \leq \eta_{ace} \leq 1$.

The ASB is a two dimensional adaptive detection algorithm consisting of a first stage AMF detection followed by a second stage ACE detection. The algorithm is best described pictorially as in fig(1). If the test cell \mathbf{x} produces coordinates (t_{AMF}, t_{ACE}) satisfying $t_{AMF} > \eta_{amf}$ and $t_{ACE} > \eta_{ace}$, then and only then is \mathbf{x} declared target bearing.

3. PDFS AND DEPENDENCIES AMONG STATISTICS

If we restrict attention to $\mathbf{R}_T \neq \mathbf{R}$ which satisfy the following generalized eigen-relation (GER) with respect to the target array response vector \mathbf{v}

$$\mathbf{R}^{-1} \mathbf{v} = \lambda \cdot \mathbf{R}_T^{-1} \mathbf{v} \quad (4)$$

then it can be shown [5] that the distributions of the decision statistics are in general dependent upon the eigenvalues of the *color matrix*

$$\mathbf{C} \triangleq \mathbf{R}^{-1/2} \mathbf{R}_T \mathbf{R}^{-1/2}. \quad (5)$$

This matrix provides a measure of the color remaining in the process $\mathbf{R}^{-1/2} \mathbf{x}$. If $\mathbf{R}_T = \mathbf{R}$, then $\mathbf{C} = \mathbf{I}$ and the process $\mathbf{R}^{-1/2} \mathbf{x}$ is white, *i.e.* without color. Further discussion of this GER constraint is given in Section 6.

Let

$$\begin{aligned} \tilde{t}_{GLRT} &\triangleq t_{GLRT}/(1 - t_{GLRT}), & \tilde{t}_{ACE} &\triangleq t_{ACE}/(1 - t_{ACE}), \\ \tilde{\eta}_{glrt} &\triangleq \eta_{glrt}/(1 - \eta_{glrt}), & \tilde{\eta}_{ace} &\triangleq \eta_{ace}/(1 - \eta_{ace}) \\ K &\triangleq L - N + 2. \end{aligned}$$

When eq(4) holds, the statistical summary we seek is given by¹

Distributions of Adaptive Detectors

$$t_{AMF} \stackrel{d}{=} F_{1,K-1}(\tilde{\delta}_\beta) \cdot \left[(\lambda - 1) + \frac{1}{\beta} \right] \quad (6)$$

$$\tilde{t}_{GLRT} \stackrel{d}{=} F_{1,K-1}(\tilde{\delta}_\beta) \cdot [\beta(\lambda - 1) + 1]$$

$$\tilde{t}_{ACE} \stackrel{d}{=} F_{1,K-1}(\tilde{\delta}_\beta) \cdot \left[\frac{\lambda\beta}{1 - \beta} + 1 \right]$$

where $F_{1,K-1}(\tilde{\delta}_\beta)$ is a complex non-central F distributed random variable with non-centrality parameter given by

$$\tilde{\delta}_\beta^2 \triangleq \left[\frac{\beta}{1 + \beta(\lambda - 1)} \right] \cdot |S|^2 \cdot \mathbf{v}^H \mathbf{R}^{-1} \mathbf{v}. \quad (7)$$

Concerning the random variable β , note from eq(4) that the whitened target array response vector $\mathbf{R}^{-1/2} \mathbf{v}$ is an eigenvector of the color matrix \mathbf{C} with eigenvalue given by λ . The remaining $N - 1$ eigenvectors are orthogonal to this whitened target array response direction, and their span shall be called the *noise subspace*. The distribution of the random variable β is in general dependent on the eigenvalues of the color matrix \mathbf{C} corresponding to these $N - 1$ noise eigenvectors. Let the total number of distinct noise subspace roots be given by $M \leq N - 1$, and the algebraic multiplicity of m -th distinct root be n_m . Thus, $n_1 + n_2 + \dots + n_M = N - 1$. Denote these distinct roots by $\lambda_1, \lambda_2, \dots, \lambda_M$. The pdf for the loss factor β is given by

$$P_\beta = \sum_{m=1}^M \sum_{j=1}^{n_m} \left[\frac{c_{\lambda_m}(j)(n_m - j + K)!}{(K - 1)!(n_m - j)!} \right] (1 - \beta)^{n_m - j} \quad (8)$$

$$\times \beta^{K-1} \left[\frac{1}{\lambda_m} + \beta \left(1 - \frac{1}{\lambda_m} \right) \right]^{-(n_m - j + K + 1)}$$

where $0 \leq \beta \leq 1$ and the coefficients $c_{\lambda_m}(j)$ are residues dependent on the λ_i 's. The proof of these results is detailed in [5]. The significance of these results is their quasi-generality over the homogeneous case of $\mathbf{R}_T = \mathbf{R}$.

¹The symbol $\stackrel{d}{=}$ denotes equality in distribution. If two random quantities \mathbf{A} and \mathbf{B} are identically distributed, then we write $\mathbf{A} \stackrel{d}{=} \mathbf{B}$.

4. PROBABILITIES FOR 1-D ALGORITHMS

The cumulative distribution function (cdf) for a non-central F statistic can be written as a finite sum [1]. Define

$$\psi_{N,M}(a; x) \triangleq \frac{x^N}{(1+x)^{N+M-1}} \sum_{k=0}^{M-1} \binom{N+M-1}{k+N} \cdot x^k \quad (9)$$

$$\times IG_{k+1} \left(\frac{a}{1+x} \right)$$

where $IG_m(b) = e^{-b} \sum_{k=0}^{m-1} b^k/k!$ is the incomplete Gamma function. The conditional PD expressions (conditioned on the loss factor β) can be written

$$\begin{aligned} \text{PD}_{AMF|\beta} &= 1 - \psi_{1,K-1} \left[\tilde{\delta}_\beta^2; \frac{\eta_{amf}\beta}{1+\beta(\lambda-1)} \right] \\ \text{PD}_{GLRT|\beta} &= 1 - \psi_{1,K-1} \left[\tilde{\delta}_\beta^2; \frac{\tilde{\eta}_{glrt}}{1+\beta(\lambda-1)} \right] \quad (10) \\ \text{PD}_{ACE|\beta} &= 1 - \psi_{1,K-1} \left[\tilde{\delta}_\beta^2; \frac{\tilde{\eta}_{ace}(1-\beta)}{1+\beta(\lambda-1)} \right]. \end{aligned}$$

The *a priori* (unconditional) PD's are given by the integrals

$$\text{PD}_{(\cdot)} = \int_0^1 P_\beta \text{PD}_{(\cdot)|\beta} d\beta \quad (11)$$

where $(\cdot) = \text{AMF}, \text{GLRT}$ or ACE , and where P_β is given in eq(8). These results generalize those found in [1]–[3] to the case of $\mathbf{R}_T \neq \mathbf{R}$ subject to the GER.

The PFAs follow from the above PD expressions by simply setting $\tilde{\delta}_\beta = 0$, which follows when no target signal is present, *i.e.* $S = 0$.

5. PROBABILITIES FOR THE ASB 2-D ALGORITHM

Note from fig(1) that the PD for the ASB algorithm, assuming hypothesis H_1 is true, is given by

$$\text{PD}_{ASB} = Pr(t_{ACE} > \eta_{ace}, t_{AMF} > \eta_{amf}). \quad (12)$$

The decision statistics are in general dependent random variables, as implied by eq(3), and computation of PD_{ASB} must account for this. Their statistical dependencies are summarized in eq(6). *Note from eq(6) that each detector can be written equal in distribution to a function of the same two dependent random variables: $F_{1,K-1}(\tilde{\delta}_\beta)$ and β .* This observation allows for direct evaluation of the PD and PFA of the ASB detection algorithm [5]. Define the variable

$$\gamma(\eta_{ace}, \eta_{amf}) \triangleq \frac{\tilde{\eta}_{ace}}{\tilde{\eta}_{ace} + \eta_{amf}} = \frac{\eta_{ace}}{\eta_{ace} + \eta_{amf}(1 - \eta_{ace})}. \quad (13)$$

Recalling the dynamic ranges $\eta_{amf} \geq 0$ and $0 \leq \eta_{ace} \leq 1$, note that $0 \leq \gamma(\eta_{ace}, \eta_{amf}) \leq 1$ always. The sought PD

can be shown to be

$$\begin{aligned} \text{PD}_{ASB} &= \int_0^{\gamma(\eta_{ace}, \eta_{amf})} P_\beta d\beta \cdot \text{PD}_{ACE|\beta} \\ &+ \int_{\gamma(\eta_{ace}, \eta_{amf})}^1 P_\beta d\beta \cdot \text{PD}_{AMF|\beta} \end{aligned} \quad (14)$$

where the conditional quantities $\text{PD}_{(\cdot)|\beta}$ are explicitly defined in eq(10) and P_β is given in eq(8).

Note also that the PFA for the ASB is obtained from eq(14) by simply assuming that hypothesis H_0 is now true rather than H_1 , *i.e.* setting $\tilde{\delta}_\beta = 0$ which leads to:

$$\begin{aligned} \text{PFA}_{ASB} &= \int_0^{\gamma(\eta_{ace}, \eta_{amf})} P_\beta d\beta \cdot \text{PFA}_{ACE|\beta} \\ &+ \int_{\gamma(\eta_{ace}, \eta_{amf})}^1 P_\beta d\beta \cdot \text{PFA}_{AMF|\beta} \end{aligned} \quad (15)$$

where the conditional quantities $\text{PFA}_{(\cdot)|\beta}$ are implicitly defined by eq(10).

6. THE GER CONSTRAINT AND ADAPTIVE NULLING

The GER was imposed to keep analysis tractable in [5] and lead to the results reported in the preceding sections. We show that non-homogeneities can be modeled in spite of the constraints the GER imposes on the parameters \mathbf{R} , \mathbf{R}_T , and \mathbf{v} . We show this by examining the statistics of the minimum variance distortionless response (MVDR) beamformer [6].

Consider two MVDR beamformers whose clairvoyant (known covariance) weights are given by

$$\mathbf{w}_T = \mathbf{R}_T^{-1} \mathbf{v} / (\mathbf{v}^H \mathbf{R}_T^{-1} \mathbf{v}), \quad \mathbf{w} = \mathbf{R}^{-1} \mathbf{v} / (\mathbf{v}^H \mathbf{R}^{-1} \mathbf{v}) \quad (16)$$

and whose sample covariance based (SCB) adaptive weights are respectively given by

$$\hat{\mathbf{w}}_T = \hat{\mathbf{R}}_T^{-1} \mathbf{v} / (\mathbf{v}^H \hat{\mathbf{R}}_T^{-1} \mathbf{v}), \quad \hat{\mathbf{w}} = \hat{\mathbf{R}}^{-1} \mathbf{v} / (\mathbf{v}^H \hat{\mathbf{R}}^{-1} \mathbf{v}) \quad (17)$$

where

$$\hat{\mathbf{R}}_T = \mathbf{X}_T \mathbf{X}_T^H / L \quad \text{and} \quad \hat{\mathbf{R}} = \mathbf{X} \mathbf{X}^H / L. \quad (18)$$

The adaptive weight vector with the subscript “ T ” represents an MVDR beamformer trained with data homogeneous with the test cell \mathbf{x}_T . The adaptive weight vector without a subscript is trained with data whose covariance is given by $\mathbf{R} \neq \mathbf{R}_T$. Thus, the performance of the second beamformer represents the inhomogeneous case and is of interest.

The clairvoyant beam responses are defined as $b_T(\theta) = \mathbf{w}_T^H \mathbf{d}(\theta)$ and $b(\theta) = \mathbf{w}^H \mathbf{d}(\theta)$ where $\mathbf{d}(\theta)$ is an array response vector parameterized by the (azimuth) look direction θ . The magnitude squared $|b(\theta)|^2$ as a function of θ

is called the beampattern. Let the adaptive SCB beam responses and beamformer outputs be respectively denoted by

$$\begin{aligned} \hat{b}_T(\theta) &= \hat{\mathbf{w}}_T^H \mathbf{d}(\theta) & \hat{b}(\theta) &= \hat{\mathbf{w}}^H \mathbf{d}(\theta) \\ \hat{y}_T &= \hat{\mathbf{w}}_T^H \mathbf{x}_T & \hat{y} &= \hat{\mathbf{w}}^H \mathbf{x}_T. \end{aligned} \quad (19)$$

A simple case of considerable interest is

$$\mathbf{R}_T = \mathbf{R} + \mathbf{q}\mathbf{q}^H \sigma_J^2 \quad (20)$$

where the test cell \mathbf{x} has a surprise discrete unrepresented in training data of the MVDR beamformer $\hat{\mathbf{w}}$. It can be shown from results appearing in [6] that (i) the mean and variance of the adaptive null formed by the beamformer $\hat{\mathbf{w}}_T$ on the discrete \mathbf{q} are inversely proportional to the jammer's power σ_J^2 whereas the beamformer $\hat{\mathbf{w}}$ has a beam response in the direction of \mathbf{q} with mean and variance independent of σ_J^2 and therefore forms no null, and (ii) the variance of the beamformer output \hat{y} grows linearly with the jammer's power due to the absence of null formation by the beamformer $\hat{\mathbf{w}}$.

When the GER constraint is imposed it can be shown that the mean of the adaptive null on the discrete \mathbf{q} formed by beamformer $\hat{\mathbf{w}}_T$ can be chosen to be zero, *i.e.* $E\{\hat{\mathbf{w}}_T^H \mathbf{q}\} = 0$, and the resulting variance of this null is given by the expression

$$\text{Var}(\hat{\mathbf{w}}_T^H \mathbf{q}) = \frac{1}{L - N + 1} \cdot \frac{\mathbf{q}^H \mathbf{R}^{-1} \mathbf{q}}{\mathbf{v}^H \mathbf{R}^{-1} \mathbf{v}} \cdot \frac{1}{(1 + \sigma_J^2 \mathbf{q}^H \mathbf{R}^{-1} \mathbf{q})}, \quad (21)$$

which is clearly inversely proportional to the jammer's power σ_J^2 . In addition the variance of the beamformer output \hat{y} is given by

$$\frac{1}{\mathbf{v}^H \mathbf{R}^{-1} \mathbf{v}} \left[\frac{L}{L - N + 1} \right] + \frac{1}{(L - N + 1)} \cdot \frac{\mathbf{q}^H \mathbf{R}^{-1} \mathbf{q}}{\mathbf{v}^H \mathbf{R}^{-1} \mathbf{v}} \sigma_J^2 \quad (22)$$

which is clearly linear in the jammer's power σ_J^2 .

Thus, although the GER is imposed for analytic tractability it preserves the essential statistical nature of an adaptive null in the beamformer $\hat{\mathbf{w}}_T$ and avoids null formation in the beamformer $\hat{\mathbf{w}}$ allowing one to model inhomogeneities. Further details of the analysis appear in [7].

7. NUMERICAL RESULTS

Several numerical results illustrating the performance of each adaptive detection algorithm under non-homogeneous conditions will be presented at the conference. In addition numerical results illustrating the potential utility of the GER constraint for modeling inhomogeneities in adaptive processing will be presented.

REFERENCES

- [1] E. J. Kelly, "An Adaptive Detection Algorithm," *IEEE Trans. Aerosp. Electron. Syst.*, Vol. AES-22, 115 - 127 (1986).
- [2] D. E. Kreithen, A. O. Steinhardt, "Target Detection in Post-STAP Undernulled Clutter," *Proceedings of the Twenty-Ninth Asilomar Conference on Signals, Systems & Computers*, Vol. 2, pp. 1203-1207 (1995).

- [3] L. T. McWhorter, L. L. Scharf, L. J. Griffiths, "Adaptive Coherence Estimation for Radar Signal Processing," *Proceedings of the Thirtieth Asilomar Conference on Signals, Systems & Computers*, November 1996.
- [4] I. S. Reed, J. D. Mallett, L. E. Brennan, "Rapid Convergence Rate in Adaptive Arrays," *IEEE Trans. Aerospace and Electronic Systems*, Vol. AES-10, No. 6, 853-863 (1974).
- [5] C. D. Richmond, "Performance of the Adaptive Sidelobe Blanker Detection Algorithm in Non-Homogeneous Clutter," to be submitted to *IEEE Transactions on Signal Processing* 1997.
- [6] C. D. Richmond, "PDFs, Confidence Regions, and Relevant Statistics for a Class of Sample Covariance Based Array Processors," *IEEE Trans. Signal Processing*, Vol. 44, No. 7, pp. 1779-1793, July 1996.
- [7] C. D. Richmond, "Statistics of Adaptive Nulling and Modeling Inhomogeneities in Adaptive Processing," to be submitted to *IEEE Transactions on Signal Processing* 1997.
- [8] F. C. Robey, D. R. Fuhrmann, E. J. Kelly, R. A. Nitzberg, "A CFAR Adaptive Matched Filter Detector," *IEEE Trans. Aerosp. Electron. Syst.* Vol. 28, No. 1, 208-216 (1992).
- [9] S. T. Smith, "Adaptive Detector Performance in Non-Ideal Conditions," *Proceedings of the Adaptive Sensor Array Processing Workshop 14 March 1997*, MIT Lincoln Laboratory, Vol. 1, pp. 525-546.
- [10] P. A. Zulch, J. R. Guerci, "The CREST Challenge-Overview and Analysis," *Proceedings of the Adaptive Sensor Array Processing Workshop 14 March 1997*, MIT Lincoln Laboratory, Vol. 1, pp. 177-191.

FIGURES

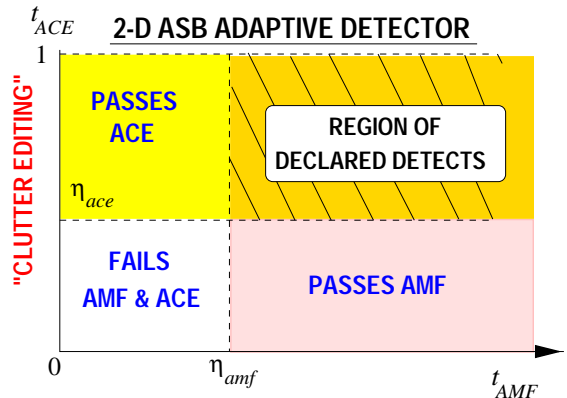


Figure 1. ASB 2-D Detection Algorithm